



# Designing an optimized free space optical (FSO) link for terrestrial commercial applications under turbulent channel conditions

Harjeevan Singh<sup>1</sup> · Rajan Miglani<sup>2</sup> · Nitin Mittal<sup>3</sup> · Surbhi Gupta<sup>1</sup> · Faisal Tubbal<sup>4,5</sup> · Raad Raad<sup>6</sup> · El Mehdi Amhoud<sup>7</sup>

Received: 28 November 2022 / Accepted: 26 March 2023 / Published online: 11 April 2023  
© The Author(s), under exclusive licence to Springer Science+Business Media, LLC, part of Springer Nature 2023

## Abstract

An abrupt surge in demand for high speed services and the advent of data-hungry frameworks such as the Internet of Things will add further to the congestion woes of the existing radio-frequency regime. Free space optical (FSO) communication technology has emerged as a promising contender to deliver high-speed data access but the performance is at times severely limited by channel turbulence. In this work, we propose an aperture averaged and optimized FSO link whose design parameters have been strategically chosen to meet the needs of diverse applications such as smart offices, smart houses, and Industry 4.0. Our investigations reveal that irrespective of channel turbulence and beam divergence profiles, the forward error correction compatible bit error rate (BER) of  $10^{-3}$  can be accomplished at the receiver at a very reasonable value of signal-to-noise ratio ranging between 20.3 and 38.2 dB. The proposed link also exhibits excellent BER stability as a change of merely of the order of  $10^2$  in BER was detected despite the worsening of channel conditions. Furthermore, in pursuit of optimizing receiver aperture size, it was found that although an aperture size of 30 cm yields improved link performance over 15 cm aperture, the latter is highly recommended for commercial applications due to its sheer ability to deliver promising BER while allowing compact design size for the receivers.

**Keywords** Commercial FSO system · Atmospheric turbulence · Beam divergence · Aperture averaging · SNR · BER

## 1 Introduction

In recent years, several multimedia applications have surged in popularity, creating large volumes of user data and necessitating the need for wireless network infrastructure having high-speed. Huge capacity, enhanced security, high quality of experience (QoE), low latency, low power consumption, and enormous device interconnection are all characteristics of the forthcoming 5G mobile networks (Morocho-Cayamcela et al. 2020). 5G

---

✉ Harjeevan Singh  
harjeevan68@gmail.com

Extended author information available on the last page of the article

communication, especially, anticipates heterogeneous networks which operate with ultra-capacity and can accommodate more users. Consequently, the data rate and the capacity of connecting wireless devices of these heterogeneous networks are very high in contrast to current wireless networks. Hence, huge-capacity-based connectivity offered by back-haul networks is required for upcoming 5G as well as future mobile networks to enable reduced delays in data transmission, high-speed, low power usage, and high-density mobile networks. Furthermore, managing a massive amount of data for 5G mobile connectivity has become extremely complex, demanding the need for resilient network infrastructure to assure the quality of service (QoS) for the end-users (Esmail et al. 2019). The Internet of Things (IoT) is a technology that allows for communications based in real-time along with various sensing applications and sharing of resources among many smart devices for several applications in the medical, social, industrial, and corporate sectors. The sudden adoption of the IoT paradigm has increased the number of physically connected smart devices exponentially (Amhoud et al. 2017). Consequently, IoT devices are generating a vast amount of data traffic, and handling this large volume of data traffic is difficult. Although the bandwidth offered by the radio frequency (RF) spectrum is limited, the usage of RF is widely recognized for supporting various applications of wireless communications. But the current electromagnetic frequency range of the RF spectrum is expected to be incapable of providing enough data rates and bandwidth for implementing IoT technology. Additionally, conventional RF technology has restricted spectrum usage along with limits imposed by frequency spectrum usage regulations. Moreover, the interference caused by other frequency signals is also one of the major limitations of communication-based on RF technology. Furthermore, the RF spectrum is currently being completely consumed by cell phone companies, television broadcasters, and communication systems based on microwave links. Because of the limitations of wireless networks employing RF technology, the researchers are carrying out investigations into wavelengths falling in the millimeter and nanometer region for offering high-speed data services (Amhoud et al. 2017). As a result, academicians and researchers have turned their focus to high-speed free space optical (FSO) links for replacing RF links. Moreover, these high-speed-based FSO links are capable of meeting the demands of future-generation cellular networks along with offering many significant characteristics such as low power consumption, low installation cost, higher data rates, low latency, and a broad range of operational frequencies (Huang et al. 2020; Singh et al. 2021).

In contrast to RF carriers, which have a limited range of frequency spectrum, optical carriers require no license to transmit data, and it makes them a viable alternative for various applications requiring huge bandwidth and high capacity. FSO links enable the transmission of the information signal between the transceivers via the atmosphere using high-frequency optical carrier signals (Singh and Mittal 2021). The line of sight (LOS) criteria should be ensured between the transceivers of the FSO link to correctly send the information signal. FSO communication has huge potential for becoming the next frontier for broadband and wireless links due to its key benefits like ultra-high transmission rates, transmission without acquiring any license, huge bandwidth, high security of data signal, compact dimensions of hardware set-up, lower power consumption, and quick installation (Chaleshtory et al. 2017). Because of its low signal beam width, FSO links operate in the visible band and infrared band of the electromagnetic spectrum. The principle of operation of FSO links is similar to optical fiber-based transmission, with the exception that the optical beam is transmitted across an unguided medium rather than a directed optical fiber. The US military used devices, powered by sunlight, to transmit telegraph signals about 50 years ago when FSO communication was first developed for applications in the space

and defense sectors. During the previous decade, FSO has become more significant for a variety of terrestrial and commercial applications. FSO links are also capable of enabling high-speed communications between LANs and MANs, offering support to mobile backhaul networks, and providing backup for optical fiber communication systems. Furthermore, FSO links can be utilized to provide high-speed and seamless connectivity for various commercial applications as shown in Fig. 1. As we can observe from Fig. 1 that FSO links can assist in providing high data services to hospitals for improving the medical services in remote areas as doctors will be able to monitor the health of patients through video conferencing (Migłani et al. 2020). To fulfill the high bandwidth requirements of commercial applications, such as 5G and IoT services for realizing smart city infrastructure, the FSO communication links are one of the main contenders, which are capable of providing seamless connectivity to the users. For example, an FSO link can provide high-speed building-to-building connectivity to enable the transmission of data at very high data rates. In addition to this, FSO links can provide high-speed data services to pedestrians and other traffic also via RF or visible light communication (VLC) links. Moreover, the FSO communications links can assist 5G-based vehicle-to-vehicle (V2V) communication for improving road safety and traffic management (Brambilla et al. 2019). The hybrid FSO/RF communication system formed by the integrating of FSO links with RF links can boost the capabilities of future networks. The hybrid FSO/RF communication system can ensure the connectivity and transmission of data in adverse weather conditions also because of possible switching between RF and FSO links (Al-eryani et al. 2018). IoT has recently emerged as a promising solution for delivering citizens of smart cities efficient services through the use of Information and Communication Technologies (ICT). FSO communications links have a lot of potential for implementing IoT services in 5G-enabled smart city infrastructure. The key commercial applications areas of IoT include intelligent transportation systems, smart homes, telemedicine, smart schools, industrial automation (Industry 4.0), smart airports, and many more (Viriyasitavat et al. 2019).



**Fig. 1** FSO links for smart city infrastructure with diverse end-users

Despite these advantages, atmospheric weather conditions have detrimental effects on FSO communication link performance (Chauhan et al. 2020). Smoke, dust, aerosols, and haze particles absorb and disperse the FSO signal. In addition to attenuation caused by tiny suspended particles in the atmosphere, atmospheric turbulence arising from variations in air density and refractive index attenuates the FSO signal and results in the degradation of the FSO link's performance. The FSO link's availability suffers greatly as a result of these degrading conditions of atmospheric medium, and the FSO link might undergo complete failure during the harsh channel conditions. As a result, the performance of these high-speed FSO links is limited by the atmospheric channel state.

The rest of the paper has been structured as follows: In Sect. 2, the previous literature on attenuation of FSO signal due to channel adversities along with the research motivation and objectives of this study will be discussed. In Sect. 3, the mathematical model to explain the channel state, atmospheric turbulence and beam divergence along with the aperture averaging technique for reducing the effects of atmospheric turbulence on FSO signals have been elaborated. The proposed FSO link for commercial as well as practical applications is discussed in Sect. 4. The discussions on the results and outcomes of this study along with the discussion on the novelty features are detailed in Sect. 5. The conclusion of this work, on the other hand, has been discussed in Sect. 6.

## 2 Related literature, research motivation and objectives

### 2.1 Related work

Along with the attenuation of the FSO beam owing to scattering, absorption, and other degrading states of the atmospheric channel, the FSO beam gets impaired due to beam divergence while it is propagating towards the FSO receiver. As a result, the FSO system's receiver will be unable to collect the incoming FSO beam properly and it will lead to beam divergence loss. The beam divergence of the optical beam has been investigated by the authors in Kaushal and Kaddoum (2017) and it has been determined that diffraction occurring near the receiver aperture results in divergence of the laser beam. The attenuation losses of the FSO link, resulting from beam divergence, rise for longer link distances unless we increase the aperture diameter of FSO receiver or advanced techniques, like receiver diversity, are implemented in the system design. Likewise, the authors in Anbarasi et al. (2017) highlight the link deterioration owing to divergence of the FSO signal and have recommended that the FSO signal should be aligned properly with the receiver telescope for reducing the losses due to divergence. Furthermore, the study conducted in Bloom et al. (2003) has pointed out the degrading characteristics of the atmosphere and concluded that controlling the atmospheric attenuation of the FSO link is not possible. However, the divergence of the FSO signal can be tweaked carefully to improve the performance of the FSO link. In addition to this, the authors have studied the loss in the power of the link in Garlinska et al. (2020) due to beam divergence, and have observed that the divergence of the FSO signal restricts the link's operational range. As a result, it becomes necessary to control the beam divergence angle during the installation time for ensuring that the FSO signal's power does not drop significantly due to beam spreading with an increase in the transmission distance. For short-range based FSO systems, a greater divergence angle of FSO signal has been suggested in Mansour et al. (2017) for eliminating misalignment errors. Furthermore, the relationship between beam divergence angle and geometrical losses has

been explored in Al-Gailani et al. (2021), with the conclusion that beam divergence should be controlled for decreasing the geometrical losses, resulting in the reduction of the FSO signal's overall attenuation losses. The precise pointing mechanism, on the other hand, has been proposed in Ghassemlooy et al. (2015) for the FSO link, having smaller angles of divergence to retain the LOS condition. In Son and Mao (2017), the authors have studied the deterioration of the system performance owing to beam divergence and proposed that the divergence angle of the FSO signal should be adjusted dynamically to improve the FSO communication system's power efficiency. Further, to improve the effectiveness of the power link budget, the aperture diameter of FSO receiver needs to be tuned according to the divergence angle of the laser beam and the transmission range. The minimal divergence angle has been promoted as a significant parameter of the FSO transmitter by the authors in Chowdhury et al. (2018). For making the installation of the FSO link easy and reliable, the large angles of beam divergence for the FSO beam were favoured in Leitgeb et al. (2004). Furthermore, the large divergence angles enable the transmission of more power while maintaining the safety of human eyes. Similarly, beam divergence has been identified as a primary obstacle in Trichili et al. (2020) for FSO links transmitting at longer ranges. The unpredictability of the FSO link along with the degradation of error probability due to atmospheric turbulence has been highlighted in Alkholidi and Altowij (2012) and a decrease in the operational range has been suggested for enhancing the system performance.

## 2.2 Research motivation and objectives

Due to burgeoning high-speed multimedia applications and a huge surge of 4G/5G mobile network users, the humongous rise in internet speeds has been portended in the near future. Additionally, the anticipated integration of the current communication network with IoT based framework for realizing the dream of smart city infrastructure has raised concerns over the bandwidth constraints of the current network infrastructure. It is anticipated that the annual data traffic will surge to approximately 1 zettabyte by the year 2022, as reported by Cisco (Forecast 2019). Furthermore, the global mobile devices will escalate to 13.1 billion and 1.4 billion devices, out of these, will be 5G compatible by the year 2023. By the same time, the total global count of smartphones (including phablets) will become 6.7 billion. The global mobile Machine-to-Machine (M2M) connections will increase to 4.4 billion by 2023, depicting the remarkable growth in the adoption of the mobile IoT paradigm (Cisco 2020).

Hence, it is apparent that the current network infrastructure, comprising the RF and microwave links, will not be able to cater to the high-speed requirements of the commercial applications, used by the end-users, and sustainably handle the global data traffic. Moreover, the high installation cost of optical fiber networks makes them economically unfit for last-mile users. Therefore, the FSO links can play an indispensable role in relieving the current network infrastructure from the woes of providing huge transmission rates and immense bandwidth.

After reviewing the limitations in the previous works, we propose an aperture averaged and optimized FSO link in this work to meet the huge bandwidth needs of the futuristic and commercial high-speed applications. Additionally, the design parameters of the transmitter and the receiver of the proposed link have been strictly configured and benchmarked with the parameters of commercial FSO systems. Unlike previous work, we have evaluated the performance characteristics of the proposed FSO link by

considering the combined impact of atmospheric attenuation, beam divergence, aperture averaging, and atmospheric turbulence to quantify the optimum combination of the beam divergence and receiver aperture diameter to configure the link for high-speed commercial applications. To optimize the FSO links for commercial applications, we feel that the comprehensive assessment of the FSO link for various receiver aperture dimensions and beam divergence profiles is extremely important as the slightest misalignment between the transceivers can result in link failure and this issue becomes even more severe in the case of smaller aperture diameters. Hence, we have further evaluated the performance of the proposed FSO link for several profiles of beam divergence and receiver aperture diameters under a host of atmospheric adversities, varying from weak to strong turbulence conditions. In this study, the performance of the proposed FSO link has been tested for various system parameters such as BER, signal-to-noise ratio (SNR), link range, and eye-patterns. Additionally, we have carried out the performance analysis of the proposed FSO link by ensuring Forward Error Correction (FEC) limit compatible bit error rate (BER) of  $10^{-3}$  at the receiver under diverse atmospheric conditions as FEC offers facilitation in the development of 100 Gbps and super 100 Gbps optical communication systems (Onohara et al. 2010d). The findings of this work provide valuable recommendations regarding the optimization of link parameters which can assist in achieving enhanced connectivity and link uptime as per the channel state. Moreover, such performance optimizations can assist telecommunication and design engineers in configuring the FSO links for commercial applications.

### 3 Mathematical modeling

In FSO communication, the information data bits are modulated onto the instantaneous intensity of the laser signal. In this work, we are considering on-off keying (OOK) modulation scheme as it is mostly employed in commercial FSO systems (Bhatnagar et al. 2016). Furthermore, the transmission of the FSO beam, based on the intensity modulation/direct detection (IM/DD) with OOK modulation scheme, takes place through the unguided medium comprising an atmospheric channel. At the receiver section, the photodetector detects the incoming optical signal and it converts the optical signal to the electrical signal, which can be explained as follows (Zhu and Kahn 2002):

$$y = xRh + n \quad (1)$$

Where  $y$  is the resulting electrical signal,  $x$  represents the transmitted intensity,  $R$  represents the responsivity of the detector, the state of the FSO channel is represented by  $h$ ,  $n$  represents the additive white gaussian noise having zero mean and variance  $\sigma_n^2$ . In this work, the thermal noise is considered as white noise because the power spectral density does not depend on the frequency (Popoola 2009). Additionally, the thermal noise follows Gaussian distribution and its variance ( $\sigma_n^2$ ) can be defined as follows (Kaiser 2003):

$$\sigma_n^2 = \frac{4kT_e B}{R_L} \quad (2)$$

Where  $k$  is the Boltzmann's constant,  $T_e$  is the temperature,  $B$  represents the bandwidth of the electrical filter, which follows the photodetector and  $R_L$  is the equivalent resistance of the receiver circuit.



### 3.1 Atmospheric path loss

The FSO signal interacts with molecular constituents of the atmospheric channel while propagating towards the receiver sections and it leads to power transmission loss of FSO signal. Beer-Lambert law can be used to describe this attenuation of FSO signals and the transmission of FSO signal through the atmospheric channel can be described as follows (Ghassemlooy et al. 2019; Kaushal et al. 2017):

$$\tau(\lambda, L) = \frac{P(\lambda, L)}{P(\lambda, 0)} = e^{-\gamma(\lambda)L} \tag{3}$$

Where  $\tau(\lambda, L)$  represents the total transmittance of the atmosphere at wavelength  $\lambda$ ,  $P(\lambda, L)$  is the optical power measured at distance  $L$  from the transmitter,  $P(\lambda, 0)$  is the optical power measured at source ( $L=0$ ), and  $\gamma(\lambda)$  represents the total attenuation coefficient per unit length. The attenuation of the FSO signal results from the scattering and absorption of the travelling beam by aerosols and molecular constituents of the atmosphere. The attenuation, resulting from aerosol or molecular absorption, is minimal for the wavelengths used for FSO communication, which comprises 780–850 nm and 1520–1600 nm. On the other hand, the attenuation of the laser signal due to scattering dominate for FSO communication. The total atmospheric attenuation, resulting from scattering and absorption, for very clear air conditions, is 0.19 dB/km. In this work, the total atmospheric attenuation of the FSO signal has been considered as 2.5 dB/km (Ghassemlooy et al. 2019; Kaushal et al. 2017).

### 3.2 Atmospheric turbulence

The characteristics of the received FSO signal are significantly affected by the atmospheric turbulence. And the turbulence in the atmosphere is generated by differences in the temperature and wind speed, which create turbulent eddies with quickly fluctuating densities, changing the optical refraction indices. The inner scale,  $l_0$ , and the outer scale,  $L_0$ , of the turbulence represent the smallest and largest turbulence eddies, respectively. When an optical beam propagates across such an inhomogeneous environment, the received optical signal’s intensities fluctuate (Singh and Mittal 2021). The changes in optical signal properties induced by scintillation vary depending on the day’s time and these changes rise sharply as the propagation distance is increased resulting in the degrading effect on BER performance. Many models, like the  $K$ -distribution model, lognormal distribution model, and Gamma-Gamma distribution model, have been widely employed to estimate the impact of turbulent atmosphere on the performance of the FSO link. However, it is critical to note that, whereas the lognormal distribution’s accuracy is confined to the scenario of weak turbulence only,  $K$ -distribution can only characterize channel conditions involving strong turbulence. According to experimental and analytical research, the Gamma-Gamma distribution model the turbulence conditions accurately from weak to high severity (Miglani et al. 2020). So, the probability density function,  $p(I)$ , of received irradiance,  $I$ , can be expressed as follows (Yang et al. 2018):

$$p(I) = \frac{2(\alpha\beta)^{(\alpha+\beta)/2}}{\Gamma(\alpha)\Gamma(\beta)} I^{\left(\frac{\alpha+\beta}{2}\right)-1} K_{\alpha-\beta} \sqrt{2\alpha\beta I} \tag{4}$$

Where  $K_n(\cdot)$  represents the modified Bessel function of 2nd kind having order  $n$ , the gamma function is represented by  $\Gamma(\cdot)$ ,  $\alpha$  and  $\beta$  are the effective number of large and small scale eddies, respectively.

### 3.3 Beam divergence

Beam divergence has an important consideration during the installation of the FSO communication links for data transmissions at high speeds. Light diffraction causes the optical beam, travelling through the atmospheric channel, to spread out (known as beam divergence). Due to this, the size of the received FSO signal becomes greater in comparison to the size of the aperture of FSO receiver. Consequently, the incoming signal does not get collected properly by the FSO receiver, resulting in beam divergence loss. Furthermore, these losses increase significantly with an increase in transmission distance of the FSO system. As a result, in practical circumstances, an appropriate divergence angle should be used for the FSO signal to get optimal link performance.

It should be noted here that the choice of appropriate beam divergence should be made for FSO applications. Most of the commercial FSO systems operate with beam divergence angles ranging between 2 and 10 mrad (Garlinska et al. 2020; Ghassemlooy et al. 2019; Bloom 2002; CableFree 2023). Although the laser source having narrow beam divergence is preferable in FSO applications, it is very challenging to operate an FSO link with a small divergence angle because of the possibility of link failure due to the slightest misalignment issues (Mansour et al. 2017). Moreover, targeting inaccuracy can decrease the received power and SNR, resulting in a higher BER and a higher likelihood of unavailability of the FSO link. In addition to this, wide divergence angles are mostly preferred in short-range-based FSO applications in order to simplify the alignment process of FSO transceivers and rule out the requirement of an active tracking system at the cost of increased geometric losses. We are analyzing the performance of the proposed commercial FSO link in this work, for beam divergence angles of 2, 4, and 6 mrad as too low divergence angle will lead to the misalignment issues and larger divergence angles will increase the beam divergence/geometric losses. The geometrical losses due to beam divergence can be given as follows (Ghassemlooy et al. 2019; Kaushal et al. 2017):

$$A_{geom} = -10 \log \left[ \frac{D_r^2}{(D_t + \phi L)^2} \right] \quad (5)$$

### 3.4 Aperture averaging

Aperture averaging has been considered a promising solution for combatting the impact of scintillation, which represents the fluctuations in the intensity of the received FSO beam as a result of atmospheric turbulence, on FSO signals (Andrews and Phillips 2005). Scintillation leads to the fading of the optical power of the received FSO signal, leading to deterioration of the system performance. In aperture averaging, the size of the receiver is kept larger in comparison to the FSO signal's wavelength, so that the detector is capable of collecting more photons. Consequently, the large size of the receiver aperture is capable of focussing a major part of the incoming FSO beam onto the area of photodetector at the receiver (Churnside 1991). Hence, the aperture averaging can reduce fading of the signal by averaging out the fluctuations in the irradiance over the size of the aperture (Agarwal



and Bansal 2019). Consequently, the scintillation of the FSO system with aperture averaging technique will be comparatively lesser in contrast to the FSO system operating with point receiver ( $D_r = 0$ ) (Vetelino et al. 2007). Apart from this, the aperture averaging reduces the variance of intensity fluctuations, given by  $\sigma_s^2(D_r)$ , for  $D_r > 0$ . The aperture averaging factor measures how much variance of intensity variations is reduced as a result of aperture averaging. We can define the aperture averaging factor,  $A$ , for quantifying the reduction in signal fading by aperture averaging as follows (Andrews and Phillips 2005):

$$A = \frac{\sigma_s^2(D_r)}{\sigma_s^2(0)} \tag{6}$$

Where  $\sigma_s^2(0)$  represent the scintillation index of the point receiver ( $D_r = 0$ ), and the aperture averaging factor,  $A$ , is further written as follows (Majumdar and Ricklin 2008):

$$A = \frac{16}{\pi D_r^2} \int_0^{D_r} b_I(\rho) \left[ \cos^{-1}\left(\frac{\rho}{D_r}\right) - \frac{\rho}{D_r} \left(1 - \frac{\rho^2}{D_r^2}\right)^{1/2} \right] \rho d\rho \tag{7}$$

Where  $\rho$  represents the separation between two points and the normalized covariance function is denoted by  $b_I(\rho)$ .

### 4 System design

In this work, we have proposed an FSO link for commercial applications and designed it using OptiSystem™ 13.0 by considering the combined impact of atmospheric attenuation, beam divergence, aperture averaging, and atmospheric turbulence. The proposed link is based on IM/DD and it employs OOK modulation scheme as most of the commercial FSO systems use IM/DD with OOK modulation technique for transmitting the data signal (Bhatnagar et al. 2016). For the proposed link, the system parameters specified in Table 1 have been configured by referring to system parameters of commercial FSO systems (Kaushal and Kaddoum 2017; Garlinska et al. 2020; Bloom 2002; CableFree 2023; Mikołajczyk et al. 2017; fSONA 2023). The system parameters of the proposed FSO link have been benchmarked with reputed literature to ensure the closeness to link conditions of the commercial and practical FSO systems. A high-frequency laser beam is used for sending the data signal through the atmosphere, which acts as an unguided channel for the optical signal. Before the transmission of the FSO beam, the message signal is modulated with a laser signal, which is the carrier signal for FSO communication. Two of the most widely utilized schemes for modulating the information signal on laser signal are direct modulation and external modulation. The direct modulation takes place inside the laser source’s resonator, and the several variations generated by different additive input components, as the laser signal’s intensity is varied, are the basis for signal modulation (Al-Gailani et al. 2021). The external modulation, on the flip side, takes place outside of the laser source’s resonator. Although we can employ a laser diode (LD) or a light-emitting diode (LED) for generating the laser signal, LDs are preferable because of their coherence, highly monochromatic nature, and directed qualities.

The proposed commercial FSO link has been depicted in Fig. 2, which has been tested under varying channel conditions. The transmitter of the proposed FSO link includes a pseudo-random binary sequence generator (PRBS), which is basically a bit sequence generator and its main role is to generate the random bit sequences. The data rate of PRBS has

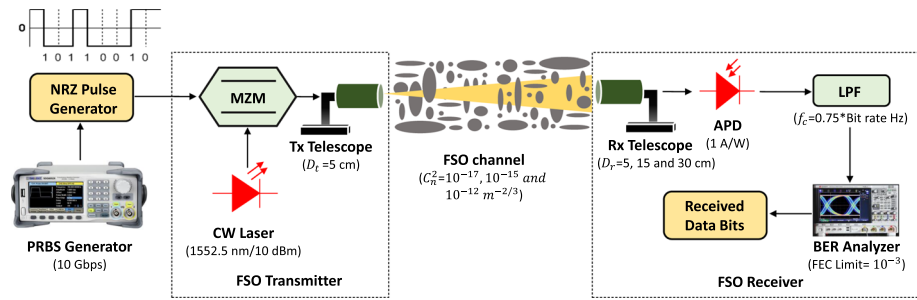


Fig. 2 System design of the proposed FSO link

**Table 1** Design parameters of the proposed FSO link (Kaushal and Kaddoum 2017; Garlinska et al. 2020; Bloom 2002; CableFree 2023; Mikołajczyk et al. 2017; fSONA 2023)

Parameter	Value
Data rate	10 Gbps
Type of laser	Continuous wave (CW)
Laser power ( $P_l$ )	10 dBm
Linewidth	10 MHz
Wavelength ( $\lambda$ )	1552.5 nm
Modulator	Mach–Zehnder Modulator
Modulation technique	OOK
Extinction ratio of modulator	30 dB
Transmitter aperture diameter ( $D_t$ )	5 cm
Optical efficiency of transmitter ( $\tau_t$ )	0.75
Turbulence Model	Gamma–Gamma model
Refractive index structure parameter ( $C_n^2$ )	$10^{-17} m^{-2/3}$ , $10^{-15} m^{-2/3}$ , and $10^{-12} m^{-2/3}$
Link range ( $L$ )	0–2 km
Beam divergence ( $\phi$ )	2–6 mrad
Receiver aperture diameter ( $D_r$ )	5–30 cm
Photodetector	APD
Responsivity of APD	1 A/W
Ionization ratio	0.9
Dark current	10 nA
Thermal noise	$100^{-24}$ W/Hz
Optical efficiency of receiver ( $\tau_r$ )	0.75

been set to 10 Gbps in this work and these bit sequences represent the information to be transmitted over the FSO channel. Furthermore, the non-return to zero (NRZ) pulse generator converts the digital data signal into the electrical domain following the bit sequence generation by PRBS. For modulating the data signal, an optical carrier signal of high frequency is produced by the laser. The laser source of the proposed link operates at a power level of 10 dBm having a wavelength of 1552.5 nm. The data signal in the electrical form, generated by the NRZ pulse generated, is further modulated with a high-frequency laser signal by the Mach-Zehnder modulator. It should be noted here that the Mach-Zehnder

modulator uses the concept of electro-optic effect for performing the modulation. Additionally, the Mach-Zehnder modulator produces high-intensity signals having high bandwidth (Prabu et al. 2015). The modulated FSO signal is transmitted through the atmosphere, acting as an unguided medium, towards the receiver and the power of the received optical signal at the receiver can be expressed as follows (Majumdar and Ricklin 2008):

$$P_r = P_t \left( \frac{D_r}{D_t + \phi L} \right)^2 \tau_t 10^{(-\alpha L/10)} \tau_r \quad (8)$$

Where  $P_r$  is the received power,  $P_t$  represents the transmitted power,  $D_t$  represents the aperture diameter of the transmitter, the aperture diameter of the receiver is given by  $D_r$ ,  $\phi$  is the divergence angle,  $L$  represents the range of the link,  $\tau_t$  is the transmitter's optical efficiency, the receiver's optical efficiency is given by  $\tau_r$ , and  $\alpha$  denotes the attenuation due to atmospheric conditions.

For this work, we have set the aperture diameter of the transmitter of the proposed FSO link as 5 cm, and the aperture diameter of the receiver has been varied from 5 to 30 cm. Similarly, the beam divergence has been varied from 2 to 6 mrad for examining the link performance up to a distance of 2 km. On the other hand, the optical efficiencies of the FSO transmitter as well as receiver have been configured as 0.75. After traversing the FSO channel, the detection process of the optical signal is carried out by an avalanche photodiode at the receiver. In addition to this, the avalanche photodiode also converts the received optical signal into an electrical form for further processing. After the detection of the FSO signal by avalanche photodiode, the signal is sent to a low pass Gaussian filter, having a cut-off frequency of  $0.75 \times \text{Bit rate}$  Hz, for removing the unwanted components present in the received signal. BER analyzer has been employed in the last stage of the proposed FSO link for analyzing the received signal's quality in the form of eye diagrams and BER.

## 5 Results and discussions

As we know that the turbulent behavior of the atmosphere impacts the performance of the FSO link, it becomes very crucial to examine the system performance under various scenarios of a turbulent atmosphere. In this work, the value of  $C_n^2$  has been taken as  $10^{-17} m^{-2/3}$ ,  $10^{-15} m^{-2/3}$ , and  $10^{-12} m^{-2/3}$  for representing weak, moderate, and strong turbulence scenarios, respectively (Ghassemlooy et al. 2019).

The received power of the proposed FSO link for various aperture diameters in case of weak, moderate, and strong turbulence scenarios have been depicted in Fig. 3 and Table 2. It can be inferred that the received power of the designed FSO system rises as the dimensions of the FSO receiver are increased. Moreover, the received power of the FSO link transmitting with a beam divergence of 6 mrad has got severely hit in contrast to 2 mrad and 4 mrad as demonstrated in Fig. 3a, b and c. For reference  $\phi$  of 4 mrad and  $D_r$  of 15 cm, the received power of the proposed link, operating with a transmission distance of 1 km, is  $-21.05$  dBm in case of a weak turbulence scenario. On the contrary, the received power of the designed FSO system drops to  $-35.93$  dBm in case of a strong turbulence scenario for the same link parameters. Hence, the proposed FSO link, operating with the link configuration of  $\phi = 4$  mrad and  $D_r = 15$  cm is capable of delivering detectable power for a link distance of 1 km in case of severe turbulence as well. So, we can conclude

**Table 2** Analysis of received power (dBm) for various channel and link design conditions

Receiver Diameter ( cm)	Atmospheric Turbulence	Received power (dBm), $L = 1$ km		
		2 mrad	4 mrad	6 mrad
5	Weak	-24.88	-30.79	-34.28
	Moderate	-25.98	-31.89	-35.38
	Strong	-39.75	-45.67	-49.15
15	Weak	-15.14	-21.05	-24.54
	Moderate	-16.24	-22.15	-25.64
	Strong	-30.01	-36.21	-39.41
30	Weak	-9.31	-15.23	-18.71
	Moderate	-10.42	-16.33	-19.82
	Strong	-24.19	-30.11	-33.59

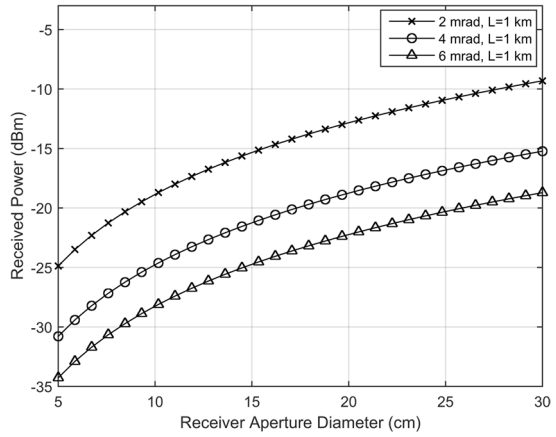
from here that  $\phi = 4$  mrad and  $D_r = 15$  cm is one of the possible link configuration, which can be further investigated for diverse channel conditions.

As depicted in Table 3, we have considered nine different cases of beam divergence angles and receiver aperture diameters to evaluate the performance characteristics of the proposed FSO link under the scenario of weak, moderate, and strong atmospheric turbulence. Cases (i-ix) depict a diverse combination of beam divergence profiles and aperture diameters of FSO receiver to be tested for the designed FSO system, under one of the given scenarios of atmospheric turbulence. In Fig. 4, the variation in the SNR of the designed system against link range has been illustrated for different angles of beam divergence and receiver aperture diameters (cases i-ix), as mentioned previously in Table 3. We can observe that the SNR of the designed FSO system drops with an increment in the operating range. Furthermore, the variation of SNR of the proposed link for various divergence angles and receiver aperture sizes (cases i-ix), corresponding to the weak, moderate, and strong scenario of turbulence, has been depicted in Fig. 4a, b and c, respectively. The beam divergence of most of the commercial FSO systems ranges from 2 to 8 mrad. However, the small beam divergence of the FSO signal is generally employed for FSO systems having an ATP mechanism for tracking the narrow FSO beam, which increases the complexity of the system along with the overall installation cost (Kaymak et al. 2018). On the other hand, larger divergence angles yield unfavorable results for FSO transmission and further make the FSO beam more vulnerable to atmospheric effects (Khalighi and Uysal 2014).

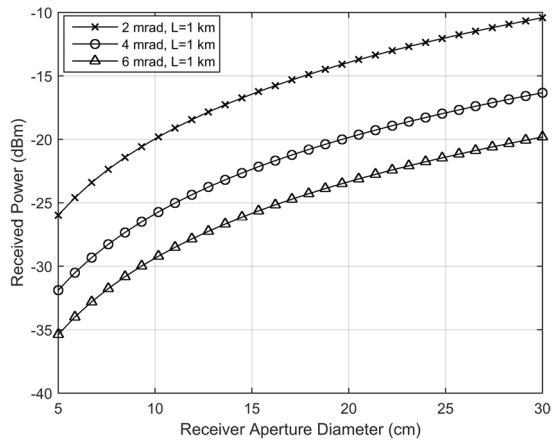
**Table 3** Different link configurations of the proposed commercial FSO link

Cases	Link parameters	Atmospheric turbulence
(i)	$\phi = 2$ mrad, $D_r = 30$ cm	Weak/Moderate/Strong
(ii)	$\phi = 4$ mrad, $D_r = 30$ cm	
(iii)	$\phi = 6$ mrad, $D_r = 30$ cm	
(iv)	$\phi = 2$ mrad, $D_r = 15$ cm	
(v)	$\phi = 4$ mrad, $D_r = 15$ cm	
(vi)	$\phi = 6$ mrad, $D_r = 15$ cm	
(vii)	$\phi = 2$ mrad, $D_r = 5$ cm	
(viii)	$\phi = 4$ mrad, $D_r = 5$ cm	
(ix)	$\phi = 6$ mrad, $D_r = 5$ cm	

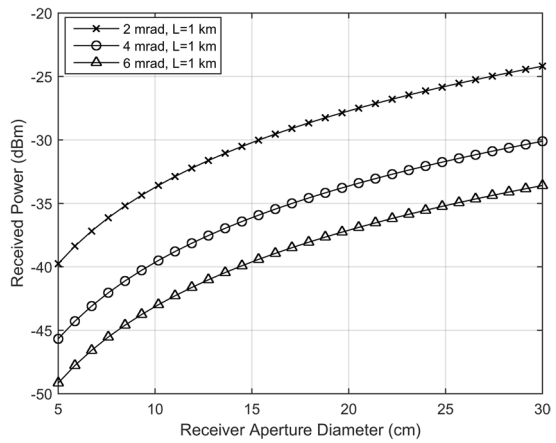
**Fig. 3** Variations in received power (dBm) for different beam divergence profiles under **a** weak turbulence; **b** moderate turbulence; **c** strong turbulence



(a)

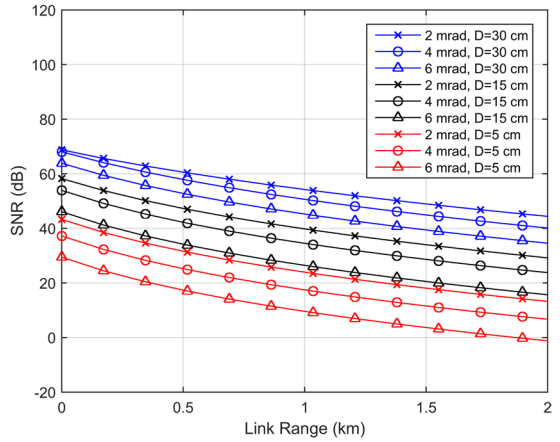


(b)

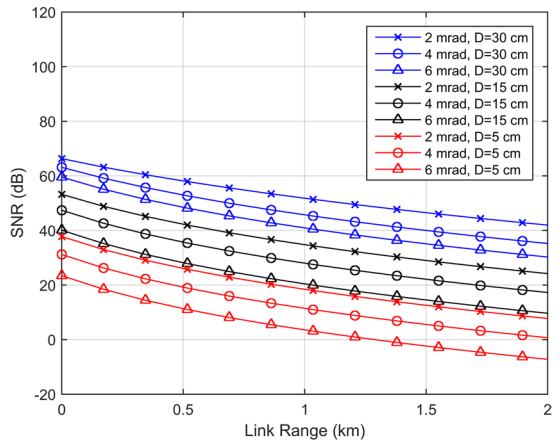


(c)

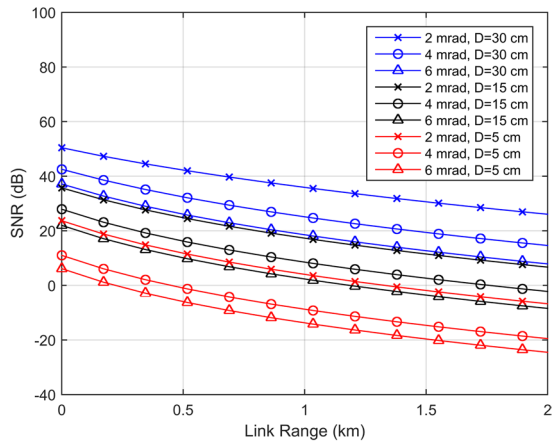
**Fig. 4** SNR ( dB) analysis for link configurations as per cases *i-ix*, under **a** weak turbulence; **b** moderate turbulence; **c** strong turbulence



(a)



(b)



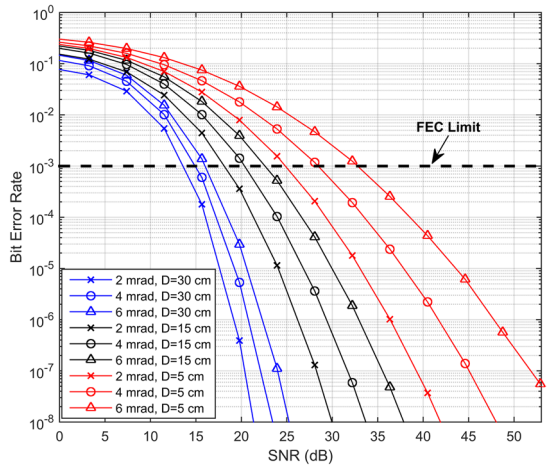
(c)



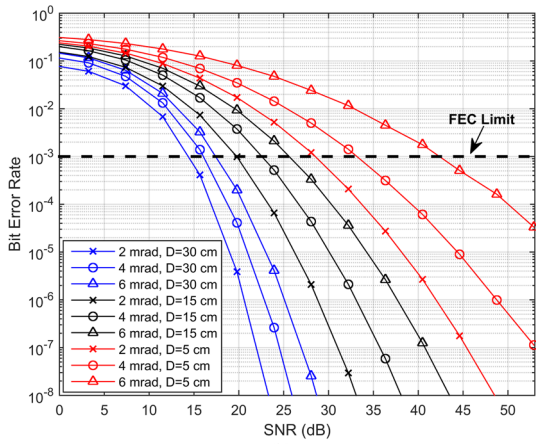
Therefore, the performance of the proposed link can be investigated for a moderate value of beam divergence, i.e.  $\phi = 4$  mrad, and different receiver aperture diameters under varied turbulence scenarios. Considering the link parameters of *case (ii)*, when  $\phi = 4$  mrad and  $D_r = 30$  cm, the proposed link has achieved an SNR of 50.2 dB, as illustrated in Fig. 4a, for an operating distance of 1 km in case of weak turbulence. On the contrary, Fig. 4b and c demonstrate the drop in the SNR of the FSO system to 45.3 dB and 24.7 dB under moderate and strong turbulence regions, respectively, for the same link parameters of the *case (ii)*. Hence, there is a drop of 9.8% in the value of SNR as we move from weak to moderate turbulence, and a 50.8% decrease in SNR values as the scenario changes from weak to strong turbulence for link configuration of *case (ii)*. Furthermore, by reducing the aperture diameter of the receiver lens to 15 cm and considering the same divergence angle of 4 mrad and transmission range of 1 km, i.e.  $\phi = 4$  mrad and  $D_r = 15$  cm (*case v*), the SNR drops by 19.1% and 76.2% as the severity of turbulence changes from weak to moderate and from weak to strong, respectively. Similarly, if the  $D_r$  is further reduced to 5 cm by retaining the  $\phi$  of 4 mrad and operating range of 1 km, i.e.  $\phi = 4$  mrad and  $D_r = 5$  cm (*case viii*), the proposed FSO link has witnessed drop of 35.3% and 154.1% with the shift of turbulence's severity from weak to moderate and then from weak to strong, respectively. So, we can conclude that the drop in SNR of the proposed FSO link is maximum in the case of a receiver lens having a diameter of 5 cm in contrast to  $D_r$  of 15 cm and 30 cm. Apart from this, the degradation in SNR of the proposed FSO link is maximum in the case of a strong turbulence scenario as compared to weak and moderate turbulence. So, the link configurations of  $\phi = 4$  mrad,  $D_r = 15$  cm and  $\phi = 4$  mrad and  $D_r = 30$  cm are capable of delivering sustainable SNR and can be recommended for commercial FSO links, but the receiver aperture diameter of 5 cm fails to achieve desired SNR under varied channel conditions. Table 4 illustrates the SNR analysis of the proposed FSO link under weak, moderate, and strong turbulence scenarios.

Figure 5 depicts the BER performance of the 1 km long proposed FSO link under varied turbulence conditions for different link configurations (*cases i-ix*) as listed in Table 3. Figure 5a, b and c highlight the BER performance of the proposed FSO link for the weak, moderate and strong turbulence scenarios, respectively. For  $D_r$  of 30 cm, the required SNR for target BER of  $10^{-3}$ , mandated to achieve the FEC limit for transmission range of 1 km is quite low under varied turbulence conditions as depicted in Fig. 5. For  $\phi = 4$  mrad and  $D_r = 30$  cm, the desired BER of  $10^{-3}$  can be achieved at SNR of 14.8 dB under weak turbulence conditions for  $L = 1$  km, and it increases to 23.2 dB for strong turbulence scenario. Similarly, the required SNR for achieving target BER in case of  $\phi = 4$  mrad and  $D_r = 15$  cm, varies from 20.3 to 38.2 dB under various turbulence scenarios (weak, moderate and strong) for  $L = 1$  km. On the contrary, the required SNR of the proposed link shoots up to very high values for  $D_r = 5$  cm under different channel conditions. For example, the target BER can be achieved, in case of  $\phi = 4$  mrad and  $D_r = 5$  cm (*case viii*), at SNR of 28.3 dB in case of weak turbulence scenario. But the required SNR for achieving BER of  $10^{-3}$  for link configuration of *case viii* becomes indeterminable as depicted in Fig. 5c. Moreover, even if we reduce the  $\phi$  from 4 to 2 mrad for  $D_r = 5$  cm, the SNR required for achieving the desired BER is 24.8 dB (in case of weak turbulence) and 50.3 dB (in case of severe turbulence). Thus, there is an increase of 102.8% in required SNR for achieving target BER for a transmission range of 1 km when the severity of turbulence changes from weak to strong for  $\phi = 2$  mrad and  $D_r = 5$  cm. So, the link configurations having receiver aperture size of 5 cm (*cases vii-ix*) are not recommended for commercial FSO systems. Table 5 shows the required SNR values for achieving target BER of  $10^{-3}$  for link range of 1 km under various turbulence conditions.

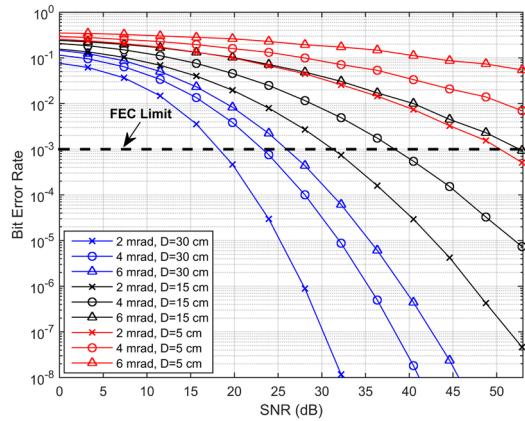
**Fig. 5** BER performance of the proposed link for configurations as per cases *i-ix*, for link range  $L = 1$  km, under **a** weak turbulence; **b** moderate turbulence; **c** strong turbulence



(a)



(b)



(c)

**Table 4** Analysis of the received SNR (dB) at the receiver for varied channel conditions

Link range (km)	Atmospheric Turbulence	SNR (dB)			SNR (dB)			SNR (dB)		
		$D_r = 5$ cm			$D_r = 15$ cm			$D_r = 30$ cm		
		2 mrad	4 mrad	6 mrad	2 mrad	4 mrad	6 mrad	2 mrad	4 mrad	6 mrad
1	Weak	23.5	17	9.1	39.3	34.1	25.9	53.8	50.2	44.8
	Moderate	17.9	11	3.1	34.3	27.6	19.9	51.4	45.3	40.5
	Strong	3.6	-9.2	-14.2	16.8	8.1	1.9	35.5	24.7	18.1
2	Weak	12.6	6.1	-1.8	28.6	23.2	15.1	43.8	39.5	33.9
	Moderate	7.1	0.1	-7.8	23.6	16.7	9.1	41.4	34.6	29.7
	Strong	-7.3	-20.1	-25.1	6.1	-2.8	-9	25.5	14	7.3

**Table 5** Required SNR (dB) at target BER of  $10^{-3}$  and  $L = 1$  km for various turbulence conditions

Atmospheric Turbulence	SNR (dB)			SNR (dB)			SNR (dB)		
	$D_r = 5$ cm			$D_r = 15$ cm			$D_r = 30$ cm		
	2 mrad	4 mrad	6 mrad	2 mrad	4 mrad	6 mrad	2 mrad	4 mrad	6 mrad
Weak	24.8	28.3	32.8	18.1	20.3	22.6	13.5	14.8	16
Moderate	28.3	33.2	42.3	19.8	22.5	25.8	14.3	16	17.3
Strong	50.3	-*	-*	31.3	38.2	52.7	18.2	23.2	25.9

\*Indeterminable values of SNR

Hence, the proposed FSO link, operating with the  $D_r = 30$  cm, has delivered excellent results for various beam divergence angles (*cases i-iii*) under varied turbulence scenarios. However, the increased aperture size of the receiver ( $D_r = 30$  cm) might be inappropriate from the design point of view and might result in a bulky receiver design. Hence, the receiver aperture of 15 cm can be recommended, along with  $\phi = 4$  mrad, for practical FSO system designs to provide seamless connectivity for various commercial applications under varied channel conditions. Moreover, the BER of the proposed FSO link increases by a factor of  $10^2$  (approx.) only for a reference SNR of 25 dB when the severity of atmospheric turbulence shifts from weak to severe, depicting the robustness of the proposed link operating with link configuration of  $\phi = 4$  mrad and  $D_r = 15$  cm.

For an operating distance of 1 km along with  $\phi = 4$  mrad, the eye diagrams of the proposed FSO link operating with a receiver lens having a diameter equal to 5 cm, 15 cm, and 30 cm, under weak, moderate and strong turbulence scenario, have been shown in Fig. 6a, b and c, respectively. The proposed FSO link is incapable of transmitting information signal, for an operating distance of 1 km, with a receiver lens diameter of 5 cm in case of weak turbulence scenario, as illustrated from almost zero opening of eye diagram in Fig. 6a. But, the performance of the link improves by increasing the receiver aperture diameter, as represented in Fig. 6b and c. Likewise, a similar trend in the performance of the proposed FSO link can be noticed from Fig. 7 for the moderate turbulence scenario as well. Further, the transmission of the proposed FSO link, operating at a range of 1 km,

gets impaired in case of a strong turbulence scenario for all receiver aperture diameters, as depicted in Fig. 8.

Table 6 demonstrates the comparison of our work with peer literature of significance, mainly based on the commercial FSO systems. The proposed FSO link, under investigation here, has a reasonable power of 10 dBm, which ensures the safety of human eyes. Furthermore, given the inverse relationship between achievable bandwidth and power of laser source, a good balance between the bandwidth and operating power levels is required in FSO link installation (Miglani et al. 2020). As a result, while the high laser power can assist in compensating the channel losses, the overall transmission capacity of the link also gets restricted by increasing the laser power. In this case, the proposed link's 10 Gbps data throughput is not only practically achievable but is also sufficient for providing higher data transmission rates to the last-mile users. Furthermore, the proposed FSO link employs an OOK modulation scheme, which is easy to implement and is widely employed in commercial FSO systems. Along with this, we have considered different turbulence scenarios (weak, moderate, and strong) for investigating the system performance of the proposed FSO link for several divergence angles and receiver aperture diameters, as mentioned in Table 3. The link parameters, considered in this work, relate to link parameters of commercial and practical FSO systems.

The majority of the commercial end-users are within a range of 1 mile from the fiber backbone network. But, it is not always feasible to provide them with access to high-speed optical connectivity, due to constraints related to difficult terrain along with the costly and time-consuming installation of the optical fiber network. Hence, the results presented in this work can be useful from a practical point of view and can be recommended for the installation of practical FSO systems to provide high data services for various commercial applications under different channel conditions.

## 6 Conclusion

In this work, we have proposed an aperture averaged and optimized commercial FSO link and its performance has been investigated under various scenarios of atmospheric channel-induced impairments and diverse link design configurations. The hallmark of the analysis presented here is that the design parameters and performance evaluation have been benchmarked such that the proposed link can ensure high-speed connectivity for end-user commercial applications. Our analysis reveals that the receiver aperture diameter of 5 cm is not suited for supporting commercial applications as the required SNR for ensuring BER of  $10^{-3}$  (FEC threshold) is quite high and non-achievable under severe channel conditions. The required SNR for achieving the target BER at  $\phi = 2$  mrad and  $D_r = 5$  cm increases by 102.8% from 24.8 to 50.3 dB as the severity of the atmospheric turbulence changes from weak to strong. It is worth mentioning here that in terms of SNR and BER, significant performance improvement is seen as the  $D_r$  increases to 30 cm. However, it is recommended that  $D_r = 15$  cm can serve as an excellent balance between the performance stability expectations and convenience of implementation as links with  $D_r = 30$  cm will expectantly fall short on the latter parameter while considering the requirement of design compactness of various futuristic commercial applications discussed in this work.

**Author Contributions** HS: Conceptualization, Methodology, Software, Formal analysis, Writing - original draft. RM: Methodology, Formal analysis, Investigation, Writing - original draft. NM: Validation, Writing

**Table 6** Comparison of proposed commercial FSO link with peer literature of significance

Comparison parameter	(Garlinska et al. 2020)	(Bloom 2002)	(CableFree 2023)	(ISONA 2023)	Proposed link	Design novelty features
Transmission power (dBm)	-20 to 26	14.9 to 33	14.8 to 19	29.03	10	The transmission power levels of the laser used in our proposed link are safe for human eyes and relevant for commercial applications
Maximum data rate (Gbps)	10	1.25	1.5	10	10	Our proposed link has delivered an encouraging data rate of 10 Gbps, which is supportable enough for futuristic high data rate applications. In addition to this, the maximum feasible data rate offered by the majority of the vendors and manufacturers of FSO systems also falls in the range of 10 Gbps (fSONA 2023)
Modulation technique	N.A	OOK	N.S	N.S	OOK	OOK modulation scheme is easy to implement practically due to its simplicity (Khalighi and Uysal 2014). The majority of the commercial FSO systems employ OOK modulation scheme for practical applications (Bhannagar et al. 2016)
Severity of turbulence	N.A	N.A	N.S	N.S	Weak, Moderate, Strong	The performance of the proposed FSO link has been tested under the impact of weak, moderate, and strong atmospheric turbulence

**Table 6** (continued)

Comparison parameter	(Garlinska et al. 2020)	(Bloom 2002)	(CableFree 2023)	(ISONA 2023)	Proposed link	Design novelty features
Beam divergence ( mrad)	2 to 10	0.5 to 4.25	(<4) to 8	N.S	2 to 6	The performance of the proposed FSO link has been evaluated by considering the beam divergence profiles (2 mrad, 4 mrad, and 6 mrad), which are mostly employed in practical as well as commercial FSO systems (Garlinska et al. 2020; Bloom 2002; Bandera 2003)
Receiver aperture diameter ( cm)	10	7.5 to 40	N.S	10	5 to 30	For investigating the performance of the proposed link, we have considered different receiver aperture diameters (5 cm, 15 cm, and 30 cm), which correspond to realistic and commercial FSO systems (Bloom 2002)
Aperture averaging	No	Yes	No	No	Yes	For improving the system performance of the proposed link under severe channel conditions of fading and attenuation, the aperture averaging technique has been adopted in this work
Forward error correction (FEC) limit	No	No	No	No	Yes	The required SNR for delivering BER of $10^{-3}$ , while ensuring FEC limit, has been calculated for various link configurations under varied channel conditions

Acronyms: N/A: Not applicable, N/S: Not specified



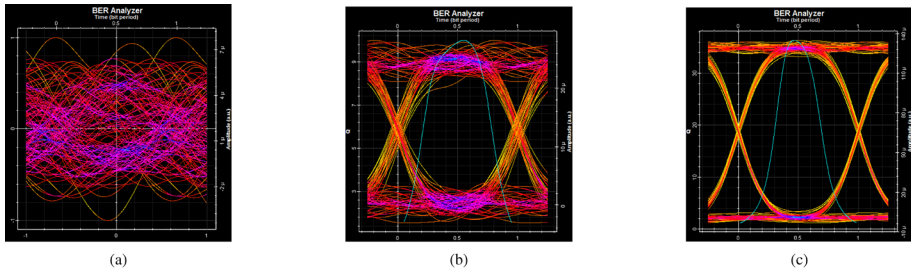


**Fig. 6** Eye diagrams as recorded at the receiver for  $L = 1$  km, beam divergence ( $\phi$ ) = 4 mrad, under weak turbulence scenario for receiver aperture diameter ( $D_r$ ) of **a** 5 cm **b** 15 cm **c** 30 cm

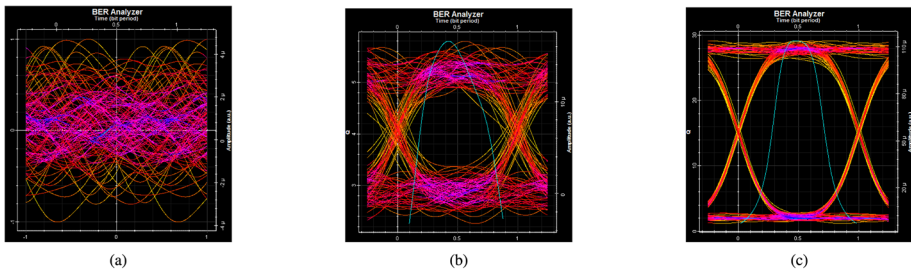


**Fig. 7** Eye diagrams as recorded at the receiver for  $L = 1$  km, beam divergence ( $\phi$ ) = 4 mrad, under moderate turbulence scenario for receiver aperture diameter ( $D_r$ ) of **a** 5 cm **b** 15 cm **c** 30 cm

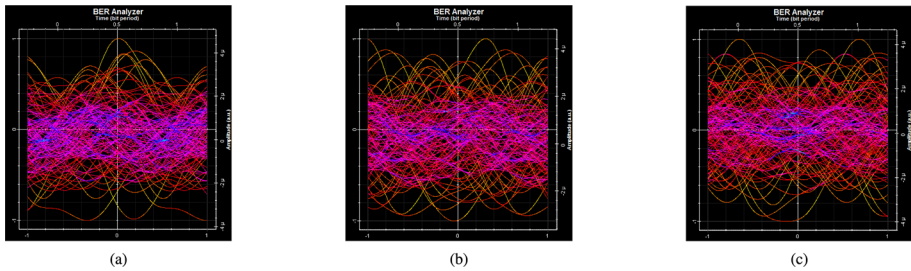


**Fig. 8** Eye diagrams as recorded at the receiver for  $L = 1$  km, beam divergence ( $\phi$ ) = 4 mrad, under strong turbulence scenario for receiver aperture diameter ( $D_r$ ) of **a** 5 cm **b** 15 cm **c** 30 cm

- Original Draft, Supervision. SG: Formal analysis, Writing - Review & Editing, Supervision. FT: Software, Formal analysis, Visualization. RR: Methodology, Writing - original draft, Supervision. EMA: Writing - Review & Editing, Visualization, Supervision.

**Funding** Not applicable

**Data availability** Not applicable

## Declarations

**Ethical approval** Not applicable

**Conflict of interest** The authors have no Conflicts of interest or Conflict of interest.

## References

- “CableFree: Free Space Optics (FSO).” Available at: <https://www.cablefree.net/cablefree-free-space-optics-fso/> (Accessed on January 10, 2023)
- “fSONA: Free Space Optical Networking Architecture.” Available at: <http://www.fsona.com/product.php?sec=10000ep> (Accessed on January 10, 2023)
- Agarwal, D., Bansal, A.: Unified error performance of a multihop DF-FSO network with aperture averaging. *J. Opt. Commun. Netw.* **11**(3), 95–106 (2019)
- Al-eryani, Y.F., Salhab, A.M., Zummo, S.A., Alouini, M.-S.: Protocol design and performance analysis of multi-user mixed RF and hybrid FSO / RF relaying with buffers. *IEEE/OSA J. Opt. Commun. Netw.* **10**(4), 309–321 (2018)
- Al-Gailani, S.A., Salleh, M.F.M., Salem, A.A., Shaddad, R.Q., Sheikh, U.U., Algeelani, N.A., Almohamad, T.A.: A survey of free space optics (FSO) communication systems, links, and networks. *IEEE Access* **9**, 7353–7373 (2021)
- Amhoud, E.M., Othman, G.R.B., Jaouen, Y.: Concatenation of space-time coding and FEC for Few-mode fiber systems. *IEEE Photonics Technol. Lett.* **29**(7), 603–606 (2017)
- Amhoud, E.M., Othman, G.R.B., Bigot, L., Song, M., E. R. Andresen, G. Labroille, M. Bigot-Astruc, and Y. Jaouën, Experimental Demonstration of Space-Time Coding for MDL Mitigation in Few-Mode Fiber Transmission Systems. In: European Conference on Optical Communication (ECOC). pp. 1 – 3. 2017
- Anbarasi, K., Hemanth, C., Sangeetha, R.G.: A review on channel models in free space optical communication systems. *Opt. Laser Technol.* **97**, 161–171 (2017)
- Andrews, L.C., Phillips, R.L.: Laser beam propagation through random media, 2nd edn. SPIE Press, Bellingham, Washington (2005)
- Bandera, P.: “Defining a Common Standard for Evaluating and Comparing Free-Space Optical Products, White paper (fSONA), pp. 1–11, (2003)
- Bhatnagar, M.R., Member, S., Ghassemlooy, Z., Member, S., Zvanovec, S., Member, S., Khalighi, M.-A., Member, S.: Quantized feedback based differential signaling for free-space optical communication system. *IEEE Trans. Commun.* **64**(12), 5176–5188 (2016)
- Bloom, S.: The physics of free-space optics. AirFiber Inc. White Paper, pp. 1–22, (2002)
- Bloom, S., Korevaar, E., Schuster, J.: Understanding the performance of free-space optics. *J. Opt. Netw.* **2**(6), 178–200 (2003)
- Brambilla, M., Matera, A., Tagliaferri, D., Nicoli, M., Spagnolini, U.: RF-Assisted Free-Space Optics for 5G Vehicle-to-Vehicle Communications. In: IEEE International Conference on Communications Workshops (ICC Workshops). Shanghai, China: IEEE., pp. 1–6 (2019)
- Chaleshtory, Z.N., Gholami, A., Ghassemlooy, Z., Sedghi, M.: Experimental investigation of environment effects on the FSO link with turbulence. *IEEE Photonics Technology Letters* **29**(17), 1435–1438 (2017)
- Chauhan, S., Miglani, R., Kansal, L., Gaba, G.S., Masud, M.: Performance analysis and enhancement of free space optical links for performance analysis and enhancement of free space optical links for developing state-of-the-art smart city framework. *Photonics* **7**(4), 132 (2020)
- Chowdhury, M.Z., Hossain, M.T., Islam, A., Jang, Y.M.: A comparative survey of optical wireless technologies: architectures and applications. *IEEE Access* **6**, 9819–9840 (2018)
- Churnside, J.H.: Aperture averaging of optical scintillations in the turbulent atmosphere. *Appl. Opt.* **30**(15), 1982–1994 (1991)
- Cisco, U.: Cisco Annual Internet Report (2018-2023). White paper, pp. 1–35, (2020)
- Esmail, M.A., Ragheb, A.M., Fathallah, H.A., Altamimi, M., Alshebeili, S.A.: 5G-28 GHz signal transmission over hybrid all-optical FSO / RF link in dusty weather conditions. *IEEE Access* **7**, 24404–24410 (2019)
- Forecast, G.M.D.T.: Cisco Visual Networking Index: Global Mobile Data Traffic Forecast Update, 2017-2022. White paper, pp. 1–33, (2019)
- Garlinska, M., PREGOWSKA, A., Masztalerz, K.: From mirrors to free-space optical communication - historical aspects in data transmission. *Future Internet* **12**(11), 1–18 (2020)
- Ghassemlooy, Z., Arnon, S., Uysal, M., Xu, Z., Cheng, J.: Emerging optical wireless communications-advances and challenges. *IEEE J. Sel. Areas Commun.* **33**(9), 1738–1749 (2015)
- Ghassemlooy, Z., Popoola, W., Rajbhandari, S.: Optical wireless communication: system and channel modeling with matlab, 2nd edn. CRC Press, Boca Raton, FL, USA (2019)

- Huang, L., Liu, S., Dai, P., Li, M., Chang, G.-K.: Unified performance analysis of hybrid FSO / RF system with diversity combining. *J. Lightwave Technol.* **38**(24), 6788–6800 (2020)
- Kaiser, G.: *Optical communications essentials*, 1st edn. McGraw-Hill Professional, New York (2003)
- Kaushal, H., Kaddoum, G.: Optical communication in space: challenges and mitigation techniques. *IEEE Commun. Surv. Tutor.* **19**(1), 57–96 (2017)
- Kaushal, H., Jain, V., Subrat, K.: *Free space optical communication*, 1st edn. Springer, New Delhi, India (2017)
- Kaymak, Y., Rojas-Cessa, R., Feng, J., Ansari, N., Zhou, M., Zhang, T.: A survey on acquisition, tracking, and pointing mechanisms for mobile free-space optical communications. *IEEE Commun. Surv. Tutor.* **20**(2), 1104–1123 (2018)
- Khalighi, M.A., Uysal, M.: Survey on free space optical communication: a communication theory perspective. *IEEE Commun. Surv. Tutor.* **16**(4), 2231–2258 (2014)
- Leitgeb, E., Gebhart, M., Birnbacher, U., Sheikh Muhammad, S., Chlestil, C.: “Applications of Free Space Optics for Broadband Access. In: *Proceedings of the Optical Networks & Technologies Conference*. Boston: Springer, pp. 579–586 (2004)
- Ikholidi, A., Altowij, K.: Effect of Clear Atmospheric Turbulence on Quality of Free Space Optical Communications in Western Asia. In: *Optical Communications Systems*. Rijeka, Croatia: Intech Open Access, (2012)
- Majumdar, A.K., Ricklin, J.: *Free-space laser communications: principles and advances*. Springer, New York, NY, USA (2008)
- Mansour, A., Mesleh, R., Abaza, M.: New challenges in wireless and free space optical communications. *Opt. Lasers Eng.* **89**, 95–108 (2017)
- Miglani, R., Malhotra, J.S., Majumdar, A.K., Tubbal, F., Raad, R.: Multi-hop relay based free space optical communication link for delivering medical services in remote areas. *IEEE Photonics J.* **12**(4), 1–21 (2020)
- Mikotajczyk, J., Bielecki, Z., Bugajski, M., Piotrowski, J., Wojtas, J., Gawron, W., Szabra, D., Prokopiuk, A.: Analysis of free-space optics development. *Metrol. Meas. Syst.* **24**(4), 653–674 (2017)
- Morocho-Cayamela, M.E., Lee, H., Lim, W.: Machine learning for 5G/B5G mobile and wireless communications: potential, limitations, and future directions. *IEEE Access* **7**, 137184–137206 (2020)
- Onohara, K., Miyata, Y., Sugihara, T., Kubo, K., Yoshida, H., Mizuochoi, T.: “Soft Decision FEC for 100G Transport Systems. In : *Conference on Optical Fiber Communication (OFC/NFOEC)*, collocated National Fiber Optic Engineers Conference, pp. 1–3 (2010)
- Popoola, W.O.: *Subcarrier Intensity Modulated Free-Space Optical Communication Systems*, Ph.D. dissertation, School Comput., Eng. Inf. Sci., Univ. Northumbria, Newcastle upon Tyn, U.K. Ph.D. dissertation, (2009)
- Prabu, K., Rajendran, R., Kumar, D.S.: Spectrum analysis of radio over free space optical communications systems through different channel models. *Optik* **126**(11–12), 1142–1145 (2015)
- Singh, H., Mittal, N.: Design and analysis of high-speed free space optical (FSO) communication system for supporting fifth generation (5G) data services in diverse geographical locations of India. *Optical and Quantum Electronics* **53**, 1–21 (2021)
- Singh, H., Mittal, N.: Analyzing the impact of fog and atmospheric turbulence on the deployment of free - space optical communication links in India. *Arab. J. Sci. Eng.* **47**(30), 2691–2710 (2021)
- Singh, H., Mittal, N., Miglani, R., Singh, H., Gaba, G.S., Hedabou, M.: Design and Analysis of High-Speed Free Space Optical (FSO) Communication System for Supporting Fifth Generation (5G) Data Services in Diverse Geographical Locations of India. *IEEE Photonics J.* **13**(5), 1–12 (2021)
- Son, I.K., Mao, S.: A survey of free space optical networks. *Digital Commun. Netw.* **3**(2), 67–77 (2017)
- Trichili, A., Cox, M.A., Ooi, B.S., Alouini, M.-S.: Roadmap to free space optics. *J. Opt. Soc. Am. B* **37**(11), 184–201 (2020)
- Vetelino, F.S., Young, C., Andrews, L., Reclons, J.: Aperture averaging effects on the probability density of irradiance fluctuations in moderate-to-strong turbulence. *Appl. Opt.* **46**(11), 2099–2108 (2007)
- Viriyasitavat, W., Bi, Z.M., Hoonsoopon, D.: Blockchain technology for applications in internet of things - mapping from system design perspective. *IEEE Internet Things J.* **6**(5), 8155–8168 (2019)
- Yang, G., Li, C., Li, J., Geng, H., Bi, M., Fan, B., Wang, T.: Performance analysis of full duplex modulating retro-reflector free-space optical communications over single and double gamma-gamma fading channels. *IEEE Trans. Commun.* **66**(8), 3597–3609 (2018)
- Zhu, X., Kahn, J.M.: Free-space optical communication through atmospheric turbulence channels. *IEEE Trans. Commun.* **50**(8), 1293–1300 (2002)

**Publisher's Note** Springer Nature remains neutral with regard to jurisdictional claims in published maps and institutional affiliations.

Springer Nature or its licensor (e.g. a society or other partner) holds exclusive rights to this article under a publishing agreement with the author(s) or other rightsholder(s); author self-archiving of the accepted

manuscript version of this article is solely governed by the terms of such publishing agreement and applicable law.

## Authors and Affiliations

Harjeevan Singh<sup>1</sup> · Rajan Miglani<sup>2</sup> · Nitin Mittal<sup>3</sup> · Surbhi Gupta<sup>1</sup> · Faisal Tubbal<sup>4,5</sup> · Raad Raad<sup>6</sup> · El Mehdi Amhoud<sup>7</sup>

Rajan Miglani  
rajanmiglani1028@gmail.com

Nitin Mittal  
mittal.nitin84@gmail.com

Surbhi Gupta  
surbhi.cgc@gmail.com

Faisal Tubbal  
faisal@uow.edu.au

Raad Raad  
raad@uow.edu.au

El Mehdi Amhoud  
Elmehdi.amhoud@um6p.ma

<sup>1</sup> Department of Electronics and Communication Engineering, Chandigarh University, Mohali 140413, India

<sup>2</sup> School of Electronics and Electrical Engineering, Lovely Professional University, Phagwara 144411, India

<sup>3</sup> Skill Faculty of Science and Technology, Shri Vishwakarma Skill University, Palwal, Haryana 121102, India

<sup>4</sup> School of Electrical, Computer and Telecommunication Engineering, University of Wollongong, Wollongong, NSW, Australia

<sup>5</sup> Technological Projects Department, The Libyan Center for Remote Sensing and Space Science, Tripoli, Libya

<sup>6</sup> School of Electrical, Computer and Telecommunication Engineering, University of Wollongong, Wollongong, NSW 2522, Australia

<sup>7</sup> School of Computer Science, Mohammed VI Polytechnic University, 43150 Benguerir, Morocco